Synthesis of Visible-Light Responsive Graphene Oxide/TiO_2 Composites with p/n Heterojunction

Chao Chen,[†,‡] Weimin Cai,[†,‡,§,*] Mingce Long,[§,*] Baoxue Zhou,[†,‡,§] Yahui Wu,[†,‡] Deyong Wu,[§] and Yujie Feng[†,‡]

[†]Department of Environmental Science and Engineering, School of Municipal and Environmental Engineering, Harbin Institute of Technology, Harbin 150090, China, [‡]State Key Laboratory of Urban Water Resource and Environment, Harbin Institute of Technology, Harbin 150090, China, and [§]School of Environmental Science and Engineering, Shanghai Jiao Tong University, Dong Chuan Road 800, Shanghai 200240, China

ABSTRACT Graphene oxide/TiO_2 composites were prepared by using $TiCl_3$ and graphene oxide as reactants. The concentration of graphene oxide in starting solution played an important role in photoelectronic and photocatalytic performance of graphene oxide/TiO_2 composites. Either a p-type or n-type semiconductor was formed by graphene oxide in graphene oxide/TiO_2 composites. These semiconductors could be excited by visible light with wavelengths longer than 510 nm and acted as sensitizer in graphene oxide/TiO_2 composites. Visible-light driven photocatalytic performance of graphene oxide/TiO_2 composites in degradation of methyl orange was also studied. Crystalline quality and chemical states of carbon elements from graphene oxide in graphene oxide/TiO_2 composites depended on the concentration of graphene oxide in the starting solution. This study shows a possible way to fabricate graphene oxide/semiconductor composites with different properties by using a tunable semiconductor conductivity type of graphene oxide.

KEYWORDS: graphene oxide · titanium dioxide · p/n heterojunction · visible light · photocatalysis

Graphene is an attractive material for fabricating graphene containing inorganic composites because of its unique electronic property,[1] high transparency,[2] flexible structure, and large theoretical specific surface area.[3] Several methods have been used to synthesize graphene, and one method consisting of oxidization of graphite, subsequent exfoliation, and reduction of graphite oxide, is widely used.[4−6] In most cases, partially oxidized graphene is favorable for its tunable optical, conductive, and chemical properties. Graphene oxide (GO) could be regarded as graphene functionalized by carboxylic acid, hydroxyl, and epoxide groups,[7] and the properties of graphene are sensitive to chemical doping, adsorbed or bound species, and structure distortion.[8] Generally an electron energy gap could be opened by oxidation of graphene,[9] and the value of the energy gap depends on oxidization degree of graphene and species of oxygen containing groups.[9] It means GO could change from conducting to insulating by tuning the C/O ratios.[9,10] Moreover, graphene oxide has been found to be either a p-type or n-type semiconductor.[11,12] In addition, oxidation of graphene could cause structure distortion of graphene.[13] Therefore different oxidation degrees of graphene would result in a diverse energy gap and structure distortion, and then cause different chemical properties of graphene. Literatures show that decorating inorganic materials with modified graphene could enhance their electronic,[3,10] electrocatalytic,[4,14] and photocatalytic[6,15] properties.

TiO_2 has been widely studied in the fields of energy conversion[16,17] and pollutant degradation[18] owing to its effectiveness, cheapness, and chemical stability. In recent years much effort has been exerted on constructing visible-light driven TiO_2 because of its obvious merit on the solar energy utilization. Modifying TiO_2 with a carbonaceous substance on the surface can induce visible light responsive activity.[19−21] Various types of carbon, such as graphitic or coke-like carbon[20,21] or carbonate structural fragments bonding with titanium[22] are proposed as the origin of the visible light activity. Therefore, it can be inferred that ordered nanostructure carbonaceous materials with tunable property could be used to modify the TiO_2 surface to contrive visible-light responsive materials. If this can be realized, it will facilitate explicit and systematic study on the mechanism of action of carbon coated on the TiO_2 surface. Graphene and graphene oxide with tunable property shed new light on this. However, as far as we know, the reported literatures about graphene or graphene

*Address correspondence to wmcai@sjtu.edu.cn, long_mc@sjtu.edu.cn.

Received for review June 9, 2010 and accepted October 04, 2010.

Published online October 14, 2010. 10.1021/nn102130m

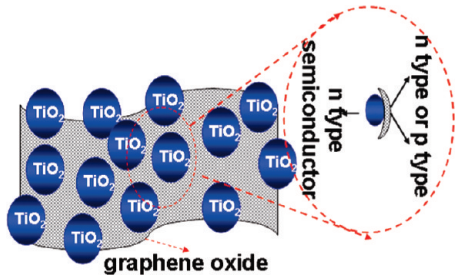

Scheme 1. Graphene oxide/TiO_2 composites (GOT) with graphene oxide existing as either n type or p type semiconductor.

oxide/TiO_2 composites only focus on photogenerated electron transfer between TiO_2 and graphene/graphene oxide,[6,23−25] Li-ion insertion/extraction,[10] and effect of graphene adsorption property on TiO_2 photocatalytic performance.[6,26]

There is still little work focusing on using tunable chemical properties of graphene oxide to construct graphene oxide/TiO_2 composites (GOT) for visible light driven photocatalytic or photoelectrochemical application. Herein we synthesize GOT by using graphene oxide and $TiCl_3$ as reactants with different GO concentration in starting solution. Either p type or n type semiconductor behavior has been observed for GO in composites, which could act both as sensitizer and electron carrier. The composite is shown in Scheme 1. Existence of a p/n heterojunction in GOT has been found. The effect of the starting solution compositions on photoelectronic and photocatalytic activity of GOT has been studied in detail.

RESULTS AND DISCUSSION

Characterization of GOT and GO. The self-assembly method[10] reported elsewhere with some modification was used to prepare graphene oxide/TiO_2 composites. $TiCl_3$ and graphene oxide were used as reactants. The starting solution composition is known to play an important role in material property. Therefore, starting solutions with different graphene oxide concentrations were used during preparation of graphene oxide/TiO_2 composites. The obtained composites were named

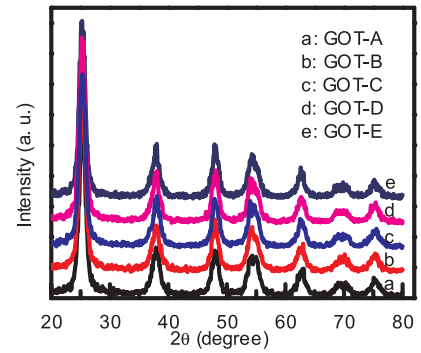

Figure 2. XRD patterns of graphene oxide/TiO_2 composites (GOT).

from GOT-A to GOT-E as the concentration of GO in the starting solution increased. According to element analysis, carbon element contents of GOT-A, GOT-B, GOT-C, GOT-D, and GOT-E are 0.14, 0.15, 0.13, 0.25, and 0.51 wt %, respectively.

Atomic force microscopy (AFM) was used to analyze GO (Figure 1). The height of GO is about 0.8 nm from cross sectional analysis (Figure 1b). This value is almost the same as the interlayer spacing (0.78 nm) of GO measured by X-ray powder diffraction (XRD) (Supporting Information Figure S1). These results suggest that exfoliation of graphite oxide down to single-layer sheets (GO) is successfully achieved.[27,28] XRD patterns of GOT-A, GOT-B, GOT-C, GOT-D, and GOT-E (Figure 2) suggest pure anatase phase of TiO_2 (JPCDS card: 73-1764). Crystal sizes calculated with Scherer formula based on the full width at half-maximum of the peak at 25.4° are in the range from 6 to 8 nm.

Raman is a powerful tool to characterize the crystalline quality of carbon.[8,29] The Raman spectrum of GO (inset graph in Figure 3A) shows the presence of D, G, and 2D bands at 1340, 1585, and 2701 cm^{-1}, respectively. G band is common to all sp2 carbon forms[30] and provides information on the in-plane vibration of sp2 bonded carbon atoms.[31] The D band suggests the presence of sp3 defects.[32] The 2D band, which originates from a two-phonon double resonance Raman process,[32] provides information on the stacking order[33] of gra-

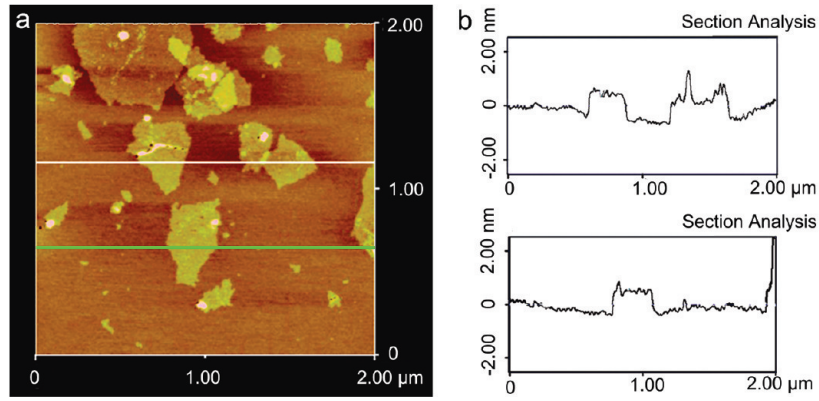

Figure 1. Tapping-mode AFM image of graphene oxide (a) and corresponding height profiles (b). The upper inset and lower inset in graph b correspond to topography height profiles along the white line and green line in graph a, respectively.

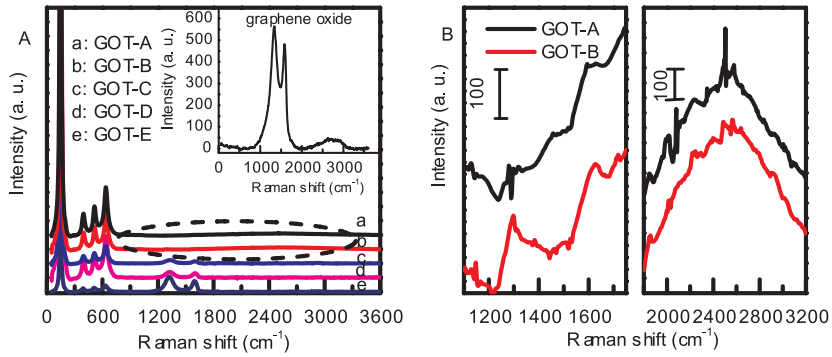

Figure 3. Raman spectra of (A) graphene oxide/TiO_2 composites (GOT) and graphene oxide and (B) magnified Raman spectra corresponding to the region marked with dash lines in graph A.

phitic sp2 materials. The intensity of D band is stronger than that of G band and this indicates[32] the presence of high density of defects and structural disorder in GO. The shape of the 2D band is sensitive to the number of layers[34] of graphene and chemical doping.[35] Moreover, the weak and broad 2D band also suggests the existence of disorder.[36] When GO combines with TiO_2, the crystal structure of carbon changes obviously. Magnified Raman spectra of GOT-A and GOT-B (Figure 3B) show weak D and G bands. The G bands shift upward (25 cm^{-1}), and humps between 1750 and 3200 cm^{-1} (Figure 3B) centering around 2500 cm^{-1} are also observed. Although the center of these humps is different from that of the 2D band of graphene oxide, we tentatively ascribe these humps to 2D bands. It has been reported that chemical doping could cause shift of 2D band, however, the shift might not be so large, which is smaller than that of G band.[35,37] It is reported that stress could cause larger peak shift of 2D band compared with that of G band.[37] Therefore, it can be inferred that stress induced by TiO_2 nanocrystals grown on surface would result in the peak shift (around 200 cm^{-1}). However, this conclusion does not exclude the contribution of chemical doping on the peak shift. Raman spectra of GOT-C, GOT-D, and GOT-E show D band and G band around 1325 and 1600 cm^{-1}, respectively. It can be seen that D bands and G bands in GOT-C, GOT-D, and GOT-E shift downward and upward compared with that of GO, respectively. However, 2D bands could not be observed. Different Raman spectra of GOT suggest different crystalline qualities of carbon in GOT. In addition, peaks around 144, 399, 513, and 639 cm^{-1} ascribed to anatase TiO_2[38] are also observed in Raman spectra of GOT.

The high resolution-transmission electron microscopy (HRTEM) image of GO shown in Figure 4a displays flake-like shapes of GO[29] with wrinkles. The TEM image of GO with high magnification (inset of Figure 4a) confirms the disordered nature of GO as described elsewhere.[29] Selected area electron diffraction (SAED) patterns of GOT-A and GOT-E show that crystal lattice fringes observed in Figure 4b and Figure 4c originate from anantase TiO_2.

UV−vis diffuse reflectance spectra (DRS) of GOT have been recorded (Figure 5) and converted into corresponding absorption spectra by using the Kubelka−Munk function. The absorption edges of GOT-A, GOT-B, GOT-C, GOT-D, and GOT-E are almost the same and at around 400 nm, which are still in the ultraviolet light region. The corresponding band gap energy is about 3.1 eV. By comparing this band gap energy with that of P25 (3.2 eV),[39] it can be found that GOT composites do not show obvious band gap energy narrowing.

The chemical state of elements in GOT has been analyzed by X-ray photoelectron spectroscopy (XPS), and

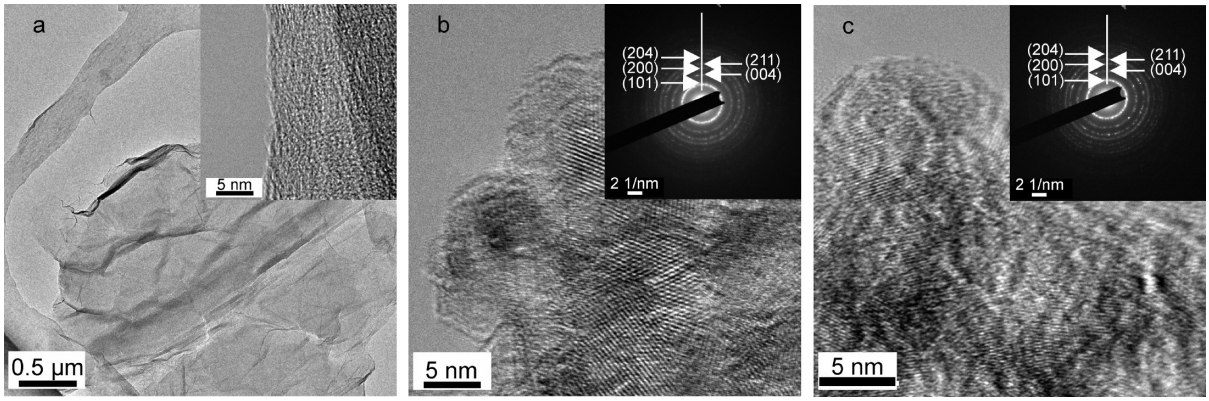

Figure 4. TEM images of graphene oxide and graphene oxide/TiO_2 composites (GOT): (a) graphene oxide, (b) GOT-A, and (c) GOT-E. The insets in graphs b and c show corresponding selected area electron diffraction patterns of GOT.

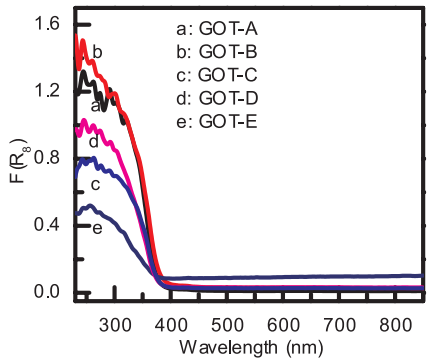

Figure 5. UV−vis absorption spectra of graphene oxide/TiO_2 composites (GOT).

the results are shown in Figure 6. The obtained data were all calibrated by using contaminant carbon at binding energy of 284.6 eV. No observable difference in binding energies of Ti or O elements among GOT-A, GOT-E, and P25 has been found (Supporting Information S2). The C 1s XPS spectrum of GO shows two peaks at 284.6 and 286.6 eV. The binding energy at 284.6 eV could be either assigned to the adventitious carbon contamination adsorbed from the ambient or assigned to the C−C bond (sp^2) of graphene.[31,40] The peak at 286.6 eV is ascribed to C−O bond,[23,31] and the O 1s XPS spectrum of GO also suggests the existence of C−O bond (Supporting Information S2), suggesting the existence of defects in GO. C 1s XPS spectra of GOT-A and GOT-E show different chemical states of carbon compared with that of GO. Two peaks (284.6 and 287.6 eV) and three peaks (284.6, 287.3, and 291.8 eV) were found for GOT-A and GOT-E, respectively. Peaks located at binding energies of 287.3 and 287.6 eV could be assigned to the existence of C═O bond.[41,42] It has been reported that the peak at 291.8 eV could be ascribed to the $\pi \rightarrow \pi^*$ satellite of the phenyl ring in the lubricant piperonyl end group,[43] one kind of oxygen modified phenyl rings. It is known that graphene oxide is composed of small aromatic conjugated domains modified with carboxylic acid, hydroxyl, and epoxide groups.[7] Therefore the peak at 291.8 eV suggests the existence

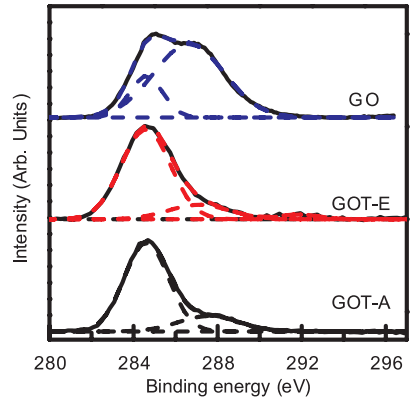

Figure 6. C 1s core-level XPS spectra of GO and graphene oxide/TiO_2 composites (GOT) GOT-A and GOT-E.

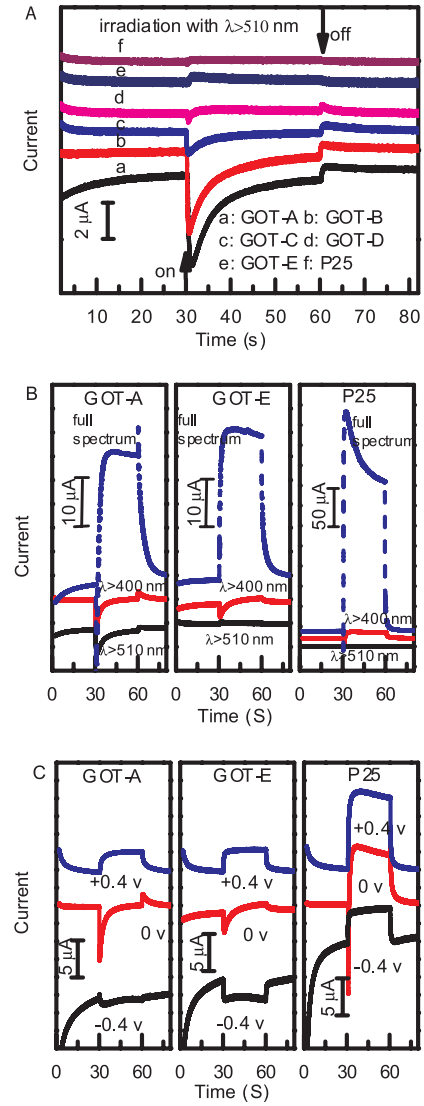

Figure 7. Transient photocurrents of graphene oxide/TiO_2 composites (GOT) and P25 (A) irradiated with a wavelength larger than 510 nm; (B) transient photocurrents of GOT-A, GOT-E, and P25 under different kinds of irradiation with an electrode potential of 0 V *vs* Ag/AgCl; (C) transient photocurrents of GOT-A, GOT-E, and P25 under irradiation above 400 nm with different electrode potential *vs* Ag/AgCl.

of a partially modified π structure in the sample GOT-E. These results suggest that there is a great effect of starting solution composition on the chemical states of carbon in GOT.

Photoelectrochemistry of GOT. Transient photocurrents of GOT and P25 under irradiation with wavelength longer than 510 nm, wavelength longer than 400 nm, and full spectrum of light source have been analyzed (Figure 7). When irradiated with wavelengths longer than 510 nm, GOT-A, GOT-B, and GOT-C possess a cathodic photocurrent (Figure 7A), which is the p-type photoresponse.[44] GOT-D and GOT-E possess anodic photocurrent[44] (Figure 7A), which is the n-type photoresponse. This phenomenon suggests different kinds of semiconductor conductivity types of graphene oxide

in GOT. In the following transient photocurrent tests, GOT-A, GOT-B, and GOT-C show an almost similar behavior, while GOT-D and GOT-E show another similar behavior. The results of GOT-A and GOT-E are representatively selected and shown in Figure 7B,C for the following discussion about GOT. When the irradiation wavelength extended to the ultraviolet light region, photocurrent conversion (Figure 7B) from cathodic to anodic was found for GOT-A, and no photocurrent conversion was found for GOT-E (Figure 7B). Wavelength dependent photocurrent conversion of GOT-A suggests formation of a p-n heterojunction.[44,45]

When GOT-A was illuminated with wavelengths longer than 400 nm or full spectrum of light source, cathodic sharp spike and anodic sharp spike appeared as light was switched on and off, respectively. This phenomenon suggests faster photocurrent generation kinetics of GO than that of TiO_2. When the light was switched on, the faster photoresponse of p-type GO caused cathodic photocurrent. Then this photocurrent was offset by anodic photocurrent generated by relative slow photoresponsive TiO_2 with the time of illumination. It is a piece of evidence that the p-type GO possess an excellent hole conductivity, which might facilitate the separation of carriers photogenerated by GOT-A during photocatalytic reaction. When the light was switched off, cathodic photocurrent due to p-type GO could disappear faster than anodic photocurrent of TiO_2. Therefore an anodic overshoot was observed.

All kinds of GOT possess photocurrent direction conversion as electrode potential ranges from −0.4 V to +0.4 V *vs* Ag/AgCl (Figure 7C) when irradiated with wavelengths longer than 400 nm. In this situation, the existence of p/n heterojunction could be used to explain photocurrent direction conversion of GOT-A.[44] However, this could not be the reason for photocurrent direction conversion of GOT-E. It can be inferred that graphene oxide in GOT-E facilitates this photocurrent conversion. The work function of graphene has been computed to be 4.42 eV,[46] which signifies possible electron transfer from the TiO_2 conduction band to graphene.[3] No literature has reported the work function of graphene oxide as far as we know. Oxidative treatment on carbon nanotubes, which could be seen as rolled up graphene sheets with a nanoscale diameter, is found to increase the work function of carbon nanotubes.[47] Therefore, we assume that graphene oxide possesses a higher work function than graphene, which makes it more possible for electrons to transfer from TiO_2 to graphene oxide. And graphene oxide has been proven to accept photogenerated electrons of TiO_2.[24] When GOT-E was irradiated, part of the photogenerated electron of TiO_2 would transfer from TiO_2 to graphene oxide. The existence of π-bands in GOT-E facilitates charge transfer along the π system[48] either to electrode or to solution. Application of a negative bias as −0.4 V *vs* Ag/AgCl electrode potential would prevent electron transfer from GOT-E to the electrode, but facilitate electron transfer from GOT-E to solution. Therefore, cathodic photocurrent could be observed, as shown in Figure 7C.

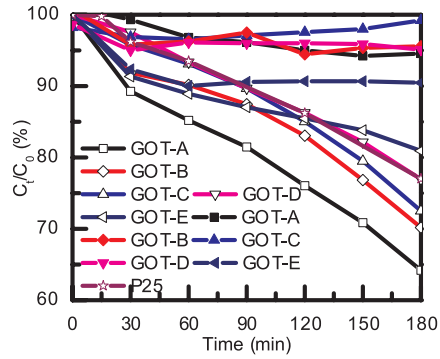

Figure 8. Degradation of methyl orange with graphene oxide/TiO_2 composites (GOT) and P25 (curves with open symbols) under irradiation above 400 nm and adsorption of methyl orange on GOT (curves with solid symbols) without irradiation (1 g/L of catalyst, 12 mg/L methyl orange).

Considering the self-assembly synthesis method used in this study,[10] $TiCl_3$ on the surface of graphene oxide is considered to undergo TiO_2 crystalline formation and crystalline growth processes. The scheme of reaction has been illustrated elsewhere.[10] It is reported that depositing metal oxides on graphene followed by annealing could induce defects and stress[37] to graphene and then change the chemical properties of graphene. GO is structurally seen as an atomically thin layer, almost similar to that of graphene. We infer that TiO_2 nanocrystals grown on the GO surface could also cause stress to GO. When the concentration of GO in the starting solution varies, the amount of TiO_2 nanocrystals grown on the surface of GO might change and the stress induced by TiO_2 to GO might change. The electrical and optical properties of GO are reported to depend on its chemical and atomic structure,[36] therefore it is inferred that the chemical property of GOT varies as the concentration of GO in the starting solution varies, and the variation of the chemical property might be the reason why semiconducting properties of GOT-A and GOT-E are different. Different Raman, XPS, and the following photocatalytic activity analysis results between GOT-A and GOT-E also prove the chemical property variation.

Photocatalytic Activity of GOT. Photocatalytic activity of GOT in decolorization of MO under irradiation above 400 nm (Figure 8) has been studied. It can be seen that visible-light photocatalytic performance of GOT and P25 decreases in the order GOT-A > GOT-B > GOT-C > GOT-D ≈ P25 > GOT-E, and GOT-E possesses the best adsorption performance. When GOT complexes were irradiated by light longer than 400 nm, both TiO_2 and semiconductor formed by GO could be excited. Although P25 possesses the largest photocurrent compared to GOT (Figure 7B), the photocatalytic perfor-

mance was smaller than that of GOT-A, GOT-B, and GOT-C. Therefore it is inferred that the semiconductor formed by GO with a band gap narrower than 2.43 eV in GOT (Figure 7A) plays an important role in the visible-light photocatalytic performance of GOT. The band gap was calculated based on the irradiation wavelength (longer than 510 nm). The p-type semiconductor formed by GO in GOT-A, GOT-B, and GOT-C might act as a sensitizer and enhance the photocatalytic performance of GOT-A, GOT-B, and GOT-C. Although an n-type semiconductor was formed by GO in GOT-D and GOT-E (Figure 7A), the photocurrent generated was negligible, and this sensitizer would not obviously enhance the visible-light photocatalytic performance of TiO_2. The results suggest a great effect of starting solution compositions during catalyst preparation on the photocatalytic performance of GOT.

CONCLUSION

Different kinds of semiconductor formed by graphene oxide (GO) in graphene oxide/TiO_2 composites (GOT) were synthesized in this study. These semiconductors formed by GO possessed band gap energies narrower than 2.43 eV. When GO formed a p-type semiconductor, a p/n heterojunction could be clearly observed. Photocatalytic activity tests showed that the semiconductors formed by GO on the surface of GOT could act as a sensitizer and enhance the visible-light photocatalytic performance of GOT. The fabrication of GOT with different kinds of sensitizers could be simply realized by changing the GO concentration in the starting solution during preparation of GOT. Although only TiO_2 is used in this study to form composites with graphene oxide, this study suggests the possibility for fabrication of hybrid semiconductors with graphene oxide and semiconductors.

METHODS

Synthesis of Graphene Oxide. Graphene oxide was synthesized from oxidation of graphite by using the Hummers method,[49] and 0.5 g of graphite is used as reactant during the synthesis of graphene oxide. The obtained graphite oxide was then dispersed in 500 mL of water and exfoliated by using a JY92-2D ultrasonic crasher (Ningbo Scientz Biotechnology Co. Ltd.) (400 W) for 40 min. Unexfoliated graphite oxide in suspension after ultrasonication was removed by using 15 min centrifugation at 3000 rpm. The obtained suspension with graphene oxide (1.3 g/L) was then used for the following synthesis of graphene oxide/TiO_2composites.

Synthesis of Graphene Oxide/TiO_2 Composites. Graphene oxide/TiO_2 composites were synthesized by using the self-assembly method reported by Wang *et al.* with some modification.[10] The synthesis method can be described as follows: graphene oxide (1.3 g/L) was diluted by water, then sodium dodecylsulfate (SDS, 0.05 mol/L) was added into the graphene oxide-containing solution. The amount of graphene oxide, water, and sodium dodecysulfate in the mixture for different kinds of graphene oxide/TiO_2 composites were listed in Table 1. Then 50 mL of $TiCl_3$ (0.12 mol/L) was added to the suspension under modest stirring. Subsequently the suspension solution was stirred for another 1 h. Then 10 mL of Na_2SO_4 (0.6 M) and 5 mL of H_2O_2 (1 wt %) were added to the solution in sequence. The obtained suspension solution was then stirred at 90 °C for 16 h. The precipitates were separated, washed with water and ethanol, dried at 70 °C, and then calcined in air at 400 °C with a heating rate of 5 K/min for 2 h. Then the obtained composites were treated with a cleaning process involving three cycles of centrifugation/washing/redispersion in water and dried at 70 °C in air.

GOT Characterization. The AFM images were obtained by using a NanoscopeIIIa scanning probe microscope (Digital Instruments, Santa Barbara, CA, USA) on a new cleaved mica surface in tapping mode in air. X-ray diffraction patterns were measured on a Rigaku D/Max-2200/PC X-ray diffractometer. Raman spectra were detected using a LabRam-1B Raman microspectrometer at 632.8 nm (Horiba Jobin Yvon, France). The morphology and structure were observed by a JEM-2100F high resolution-transmission electron microscope (HRTEM) (JEOL) operated at 200 kV. The point resolution of HRTEM is 0.19 nm. X-ray photoelectron spectroscopy measurements were carried out on a RBD upgraded PHI-5000C ESCA system (Perkin-Elmer). UV−vis diffuse reflectance spectra were measured on a TU-1901 UV−vis spectrophotometer (Beijing Purkinje General Instrument Co., Ltd., China). The carbon element contents were recorded by a Vario EL III elemental analyzer (Elementar, Germany). Photoelectrochemical test systems were composed of an CHI 600D Electrochemistry potentiostat, a 500 W xenon lamp with or without cutoff filters ($\lambda > 400$ nm or $\lambda > 510$ nm), and a homemade three-electrode cell using platinum as counter electrode, Ag/AgCl as reference electrode, and Na_2SO_4 (0.5 M) as electrolyte. GOT and P25 electrodes were prepared by depositing suspensions made of GOT or P25 and absolute ethanol (concentration of GOT or P25 is 100 g/L) onto fluorine-doped tin oxide-coated glass (FTO) using the doctor-blade coating method with a glass rod and scotch tape as a frame and spacer, respectively. Electrodes were dried and then calcined at 300 °C for 2 h. During measurements, the electrodes were pressed against an O-ring of an electrochemical cell with a working area of 3.14 cm^2.

Photocatalytic Activity. Visible-light photocatalytic activity of GOT and P25 was evaluated by degradation of methyl orange. The optical system for the test consists of a 1000 W xenon lamp and a cutoff filter ($\lambda > 400$ nm). In a typical test for MO degradation, 0.05 g of catalyst powder was added into 50 mL of methyl orange solution (12 mg/L). The suspension was then treated with ultrasonic waves for 5 min and stirred in the dark for 15 min. Then the suspension was placed under visible-light irradiation, and samples were taken, separated, and analyzed at regular time intervals with a UNICO UV-2102 spectrometer at 464 nm. The control experiment without irradiation was also conducted in order to test the adsorption performance of the catalyst.

TABLE 1. Amount of GO, SDS, and H_2O Added in Starting Solution for Preparation of GOT

GOT	GOT-A	GOT-B	GOT-C	GOT-D	GOT-E
G0 (mL)	1.85	3.7	7.4	18.5	37
SDS (mL)	0.11	0.22	0.44	1.10	2.20
H_20 (mL)	71.88	69.92	66	54.24	34.64

Acknowledgment. This work is financially supported by Sate Key Laboratory of Urban Water Resource and Environment, Harbin Institute of Technology (No. QAK201101) and National Natural Science Foundation of China (No. 20907031). The authors are grateful to Limin Sun of the Instrumental Analysis Center of Shanghai Jiao Tong University for AFM measurements and Wenfeng Shangguan of School of Environmental Science and Engineering, Shanghai Jiao Tong University for DRS measurements.

Supporting Information Available: XRD pattern of GO, Ti 2p core-level XPS spectra of GOT-A, GOT-E, and P25, O 1s core-

level XPS spectra of GOT-A, GOT-E, P25, and GO. This material is available free of charge *via* the Internet at http://pubs.acs.org.

REFERENCES AND NOTES

1. Zhi, L.; Müllen, K. A Bottom-up Approach from Molecular Nanographenes to Unconventional Carbon Materials. *J. Mater. Chem.* **2008**, *18*, 1472–1484.
2. Nair, R. R.; Blake, P.; Grigorenko, A. N.; Novoselov, K. S.; Booth, T. J.; Stauber, T.; Peres, N. M. R.; Geim, A. K. Fine Structure Constant Defines Visual Transparency of Graphene. *Science* **2008**, *320*, 1308.
3. Sun, S.; Gao, L.; Liu, Y. Enhanced Dye-Sensitized Solar Cell Using Graphene-TiO_2 Photoanode Prepared by Heterogeneous Coagulation. *Appl. Phys. Lett.* **2010**, *96*, 083113.
4. Li, Y.; Tang, L.; Li, J. Preparation and Electrochemical Performance for Methanol Oxidation of Pt/Graphene Nanocomposites. *Electrochem. Commun.* **2009**, *11*, 846–849.
5. Nethravathia, C.; Nishaa, T.; Ravishankarb, N.; Shivakumarac, C.; Rajamathi, M. Graphene−Nanocrystalline Metal Sulphide Composites Produced by a One-Pot Reaction Starting from Graphite Oxide. *Carbon* **2009**, *47*, 2054–2059.
6. Zhang, H.; Lv, X.; Li, Y.; Wang, Y.; Li, J. P25-Graphene Composite as a High Performance Photocatalyst. *ACS Nano* **2010**, *4*, 380–386.
7. Zhou, X. Z.; Huang, X.; Qi, X. Y.; Wu, S. X.; Xue, C.; Boey, F. Y. C.; Yan, Q. Y.; Chen, P.; Zhang, H. *In Situ* Synthesis of Metal Nanoparticles on Single-Layer Graphene Oxide and Reduced Graphene Oxide Surfaces. *J. Phys.Chem. C* **2009**, *113*, 10842–10846.
8. Liu, L.; Ryu, S.; Tomasik, M. R.; Stolyarova, E.; Jung, N.; Hybertsen, M. S.; Steigerwald, M. L.; Brus, L. E.; Flynn, G. W. Graphene Oxidation: Thickness-Dependent Etching and Strong Chemical Doping. *Nano Lett.* **2008**, *8*, 1965–1970.
9. Boukhvalov, D. W.; Katsnelson, M. I. Modeling of Graphite Oxide. *J. Am. Chem. Soc.* **2008**, *130*, 10697–10701.
10. Wang, D. H.; Choi, D. W.; Li, J.; Yang, Z. G.; Nie, Z. M.; Kou, R.; Hu, D. H.; Wang, C. M.; Saraf, L. V.; Zhang, J. G. Self-Assembled TiO_2-Graphene Hybrid Nanostructures for Enhanced Li-Ion Insertion. *ACS Nano* **2009**, *3*, 907–914.
11. Wu, X.; Sprinkle, M.; Li, X.; Ming, F.; Berger, C.; Heer, W. A. d. Epitaxial-Graphene/Graphene-Oxide Junction: An Essential Step towards Epitaxial Graphene Electronics. *Phys. Rev. Lett.* **2008**, *101*, 026801.
12. Gilje, S.; Han, S.; Wang, M.; Wang, K. L.; Kaner, R. B. A Chemical Route to Graphene for Device Applications. *Nano Lett.* **2007**, *7*, 3394–3398.
13. Mkhoyan, K. A.; Contryman, A. W.; Silcox, J.; Stewart, D. A.; Eda, G.; Mattevi, C.; Miller, S.; Chhowalla, M. Atomic and Electronic Structure of Graphene-Oxide. *Nano Lett.* **2009**, *9*, 1058–1063.
14. Seger, B.; Kamat, P. V. Electrocatalytically Active Graphene−Platinum Nanocomposites. Role of 2-D Carbon Support in PEM Fuel cells. *J. Phys. Chem. C* **2009**, *113*, 7990–7995.
15. Wu, J.; Shen, X.; Jiang, L.; Wang, K.; Chen, K. Solvothermal Synthesis and Characterization of Sandwich-Like Graphene/ZnO Nanocomposites. *Appl. Surf. Sci.* **2010**, *256*, 2826–2830.
16. Choi, D.; Wang, D.; Viswanathan, V. V.; Bae, I.-T.; Wang, W.; Nie, Z.; Zhang, J.-G.; Graff, G. L.; Liu, J.; Yang, Z. Li-ion Batteries from $LiFePO_4$ Cathode and Anatase/Graphene Composite Anode for Stationary Energy Storage. *Electrochem. Commun.* **2010**, *12*, 378–381.
17. Mor, G. K.; Shankar, K.; Paulose, M.; Varghese, O. K.; Grimes, C. A. Use of Highly-Ordered TiO_2 Nanotube Arrays in Dye-Sensitized Solar Cells. *Nano Lett.* **2006**, *6*, 215–218.
18. Liu, Z. Y.; Zhang, X. T.; Nishimoto, S.; Murakami, T.; Fujishima, A. Efficient Photocatalytic Degradation of Gaseous Acetaldehyde by Highly Ordered TiO_2 Nanotube Arrays. *Environ. Sci. Technol.* **2008**, *42*, 8547–8551.
19. Chen, C.; Long, M.; Zeng, H.; Cai, W.; Zhou, B.; Zhang, J.; Wu, Y.; Ding, D.; Wu, D. Preparation, Characterization, and Visible-Light Activity of Carbon Modified TiO_2 with Two Kinds of Carbonaceous Species. *J. Mol. Catal. A* **2009**, *314*, 35–41.
20. Lettmann, C.; Hildenbrand, K.; Kisch, H.; Macyk, W.; Maier, W. F. Visible Light Photodegradation of 4-Chlorophenol with a Coke-Containing Titanium Dioxide Photocatalyst. *Appl. Catal. B* **2001**, *32*, 215–227.
21. Zhang, L. W.; Fu, H. B.; Zhu, Y. F. Efficient TiO_2 Photocatalysts from Surface Hybridization of TiO_2 Particles with Graphite-like Carbon. *Adv. Funct. Mater.* **2008**, *18*, 2180–2189.
22. Ząbek, P.; Eberl, J.; Kisch, H. On the Origin of Visible Light Activity in Carbon-Modified Titania. *Photochem. Photobiol. Sci.* **2009**, *8*, 264–269.
23. Yang, N.; Zhai, J.; Wang, D.; Chen, Y.; Jiang, L. Two-Dimensional Graphene Bridges Enhanced Photoinduced Charge Transport in Dye-Sensitized Solar Cells. *ACS Nano* **2010**, *4*, 887–894.
24. Lightcap, I. V.; Kosel, T. H.; Kamat, P. V. Anchoring Semiconductor and Metal Nanoparticles on a Two-Dimensional Catalyst Mat. Storing and Shuttling Electrons with Reduced Graphene Oxide. *Nano Lett.* **2010**, *10*, 577–583.
25. Manga, K. K.; Zhou, Y.; Yan, Y.; Loh, K. P. Multilayer Hybrid Films Consisting of Alternating Graphene and Titania Nanosheets with Ultrafast Electron Transfer and Photoconversion Properties. *Adv. Funct. Mater.* **2009**, *19*, 1–6.
26. Peng, W.; Wang, Z.; Yoshizawa, N.; Hatori, H.; Hirotsu, T.; Miyazawa, K. Fabrication and Characterization of Mesoporous Carbon Nanosheets-1D TiO_2 Nanostructures. *J. Mater. Chem.* **2010**, *20*, 2424–2431.
27. Kamat, P. V. Graphene-Based Nanoarchitectures. Anchoring Semiconductor and Metal Nanoparticles on a Two-Dimensional Carbon Support. *J. Phys. Chem. Lett.* **2010**, *1*, 520–527.
28. Stankovich, S.; Dikin, D. A.; Piner, R. D.; Kohlhaas, K. A.; Kleinhammes, A.; Jia, Y.; Wu, Y.; Nguyen, S. T.; Ruoff, R. S. Synthesis of Graphene-Based Nanosheets *via* Chemical Reduction of Exfoliated Graphite Oxide. *Carbon* **2007**, *45*, 1558–1565.
29. Wang, G. X.; Yang, J.; Park, J.; Gou, X. L.; Wang, B.; Liu, H.; Yao, J. Facile Synthesis and Characterization of Graphene Nanosheets. *J. Phys. Chem. C* **2008**, *112*, 8192–8195.
30. Dresselhaus, M. S.; Jorio, A.; Hofmann, M.; Dresselhaus, G.; Saito, R. Perspectives on Carbon Nanotubes and Graphene Raman Spectroscopy. *Nano Lett.* **2010**, *10*, 751–758.
31. Zhang, W. X.; Cui, J. C.; Tao, C. A.; Wu, Y. G.; Li, Z. P.; Ma, L.; Wen, Y. Q.; Li, G. T. A Strategy for Producing Pure Single-Layer Graphene Sheets Based on a Confined Self-Assembly Approach. *Angew. Chem., Int. Ed.* **2009**, *48*, 5864–5868.
32. Lu, J.; Yang, J. X.; Wang, J.; Lim, A.; Wang, S.; Loh, K. P. One-Pot Synthesis of Fluorescent Carbon Nanoribbons, Nanoparticles, and Graphene by the Exfoliation of Graphite in Ionic Liquids. *ACS Nano* **2009**, *3*, 2367–2375.
33. Ni, Z.; Wang, Y.; Yu, T.; Shen, Z. Raman Spectroscopy and Imaging of Graphene. *Nano Res.* **2008**, *1*, 273–291.
34. Wei, D. C.; Liu, Y. Q.; Zhang, H. L.; Huang, L. P.; Wu, B.; Chen, J. Y.; Yu, G. Scalable Synthesis of Few-Layer Graphene Ribbons with Controlled Morphologies by a Template Method and Their Applications in Nanoelectromechanical Switches. *J. Am. Chem. Soc.* **2009**, *131*, 11147–11154.
35. Das, A.; Pisana, S.; Chakraborty, B.; Piscanec, S.; Saha, S. K.; Waghmare, U. V.; Novoselov, K. S.; Krishnamurthy, H. R.; Geim, A. K.; Ferrari, A. C. Monitoring Dopants by Raman Scattering in an Electrochemically Top-Gated Graphene Transistor. *Nat. Nanotechnol.* **2008**, *3*, 210–215.
36. Eda, G.; Chhowalla, M. Chemically Derived Graphene Oxide: Towards Large-Area Thin-Film Electronics and Optoelectronics. *Adv. Mater.* **2010**, *22*, 2392–2415.
37. Ni, Z. H.; Wang, H. M.; Ma, Y.; Kasim, J.; Wu, Y. H.; Shen, Z. X.

Tunable Stress and Controlled Thickness Modification in Graphene by Annealing. *ACS Nano* **2008**, *2*, 1033–1039.
38. Lei, Y.; Zhang, L. D.; Fan, J. C. Fabrication, Characterization, and Raman Study of TiO_2 Nanowire Arrays Prepared by Anodic Oxidative Hydrolysis of $TiCl_3$. *Chem. Phys. Lett.* **2001**, *338*, 231–236.
39. Grzechulska, J.; Morawski, A. W. Photocatalytic Labyrinth Flow Reactor with Immobilized P25 TiO_2 Bed for Removal of Phenol from Water. *Appl. Catal. B* **2003**, *46*, 415–419.
40. Kim, W. S.; Moon, S. Y.; Lee, J. H.; Bang, S. Y.; Choi, B.; Ham, H.; Sekino, T.; Shim, K. B. Fabrication of Single-Phase Titanium Carbide Layers from MWCNTs Using High DC Pulse. *Nanotechnology* **2010**, *21*, 055608.
41. Wild, U.; Pfänder, N.; Schlögl, R. Species Analysis of Automotive Carbon Particles: Application of XPS for Integral Analysis of Filter Samples. *Fresenium J. Anal. Chem.* **1997**, *357*, 420–428.
42. Fu, R.; Yoshizawa, N.; Dresselhaus, M. S.; Dresselhaus, G.; Joe, H.; Satcher, J.; Baumann, T. F. XPS Study of Copper-Doped Carbon Aerogels. *Langmuir* **2002**, *18*, 10100–10104.
43. Onyiriuka, E. C. AM 2001 Lubricant Film on Canasite Glass-Ceramic Magnetic Memory Disk. *Chem. Mater.* **1993**, *5*, 798–801.
44. Wang, Y.; Hao, Y.; Cheng, H.; Ma, J.; Xu, B.; Li, W.; Cai, S. The Photoelectrochemistry of Transition Metal-Ion-Doped TiO_2 Nanocrystalline Electrodes and Higher Solar Cell Conversion Efficiency Based on Zn^{2+}-Doped TiO_2 Electrode. *J. Mater. Sci.* **1999**, *34*, 2773–2779.
45. Long, M. C.; Beranek, R.; Cai, W. M.; Kisch, H. Hybrid Semiconductor Electrodes for Light-Driven Photoelectrochemical Switches. *Electrochim. Acta* **2008**, *53*, 4621–4626.
46. Czerw, R.; Foley, B.; Tekleab, D.; Rubio, A.; Ajayan, P. M.; Carroll, D. L. Substrate−Interface Interactions between Carbon Nanotubes and the Supporting Substrate. *Phys. Rev. B* **2002**, *66*, 033408.
47. Ago, H.; Kugler, T.; Cacialli, F.; Salaneck, W. R.; Shaffer, M. S. P.; Windle, A. H.; Friend, R. H. Work Functions and Surface Functional Groups of Multiwall Carbon Nanotubes. *J. Phys. Chem. B* **1999**, *103*, 8116–8121.
48. Burghard, M.; Klauk, H.; Kern, K. Carbon-Based Field-Effect Transistors for Nanoelectronics. *Adv. Mater.* **2009**, *21*, 2586–2600.
49. Hummers, W. S.; Offeman, R. E. Preparation of Graphitic Oxide. *J. Am. Chem. Soc.* **1958**, *80*, 1339.